HHS Public Access

Author manuscript

Cell Rep. Author manuscript; available in PMC 2018 May 29.

Published in final edited form as:

Cell Rep. 2018 February 06; 22(6): 1509–1521. doi:10.1016/j.celrep.2018.01.040.

Early TCR Signaling Induces Rapid Aerobic Glycolysis Enabling Distinct Acute T Cell Effector Functions

Ashley V. Menk[1,8], **Nicole E. Scharping**[1,2,8], **Rebecca S. Moreci**[1], **Xue Zeng**[1,3], **Cliff Guy**[4], **Sonia Salvatore**[5], **Heekyong Bae**[6], **Jianxin Xie**[7], **Howard A. Young**[6], **Stacy Gelhaus Wendell**[5], and **Greg M. Delgoffe**[1,2,9,*]

[1]Tumor Microenvironment Center, UPMC Hillman Cancer Center, Pittsburgh, PA 15232, USA

[2]Department of Immunology, University of Pittsburgh, Pittsburgh, PA 15213, USA

[3]Tsinghua Medical University, Beijing, China

[4]St. Jude Children's Research Hospital, Memphis, TN 38105, USA

[5]Department of Cell Biology, University of Pittsburgh, Pittsburgh, PA 15213, USA

[6]Cancer and Inflammation Program, National Cancer Institute, Frederick, MD 21701, USA

[7]Cell Signaling Technology, Inc., Danvers, MA 01923, USA

SUMMARY

To fulfill bioenergetic demands of activation, T cells perform aerobic glycolysis, a process common to highly proliferative cells in which glucose is fermented into lactate rather than oxidized in mitochondria. However, the signaling events that initiate aerobic glycolysis in T cells remain unclear. We show T cell activation rapidly induces glycolysis independent of transcription, translation, CD28, and Akt and not involving increased glucose uptake or activity of glycolytic enzymes. Rather, TCR signaling promotes activation of pyruvate dehydrogenase kinase 1 (PDHK1), inhibiting mitochondrial import of pyruvate and facilitating breakdown into lactate. Inhibition of PDHK1 reveals this switch is required acutely for cytokine synthesis but dispensable for cytotoxicity. Functionally, cytokine synthesis is modulated via lactate dehydrogenase, which

*Correspondence: gdelgoffe@pitt.edu.
[8]These authors contributed equally
[9]Lead Contact

SUPPLEMENTAL INFORMATION

Supplemental Information includes Supplemental Experimental Procedures and six figures and can be found with this article online at https://doi.org/10.1016/j.celrep.2018.01.040.

AUTHOR CONTRIBUTIONS

A.V.M. performed biochemical and metabolic flux assays, as well as *in vitro* T cell functional experiments; analyzed data; and wrote the manuscript. N.E.S. performed functional *in vitro* and *in vivo* experiments, analyzed data, and wrote the manuscript. R.S.M. performed the initial Seahorse assays and assisted with *in vivo* experiments. X.Z. performed immunoprecipitation experiments in HEK293T cells. C.G. performed TIRF microscopy experiments. S.S. performed extractions and analysis for isotopic flux analysis. H.B. assisted with ARE-deficient mouse experiments. J.X. generated the anti-phospho-PDHK1 (Y243) antibody. H.A.Y. originally generated and provided the ARE-mutant animals. S.G.W. oversaw metabolic tracing experiments. G.M.D. designed and performed the experiments, analyzed data, oversaw research, and wrote the manuscript.

DECLARATION OF INTERESTS

J.X. is an employee of Cell Signaling Technology.

represses cytokine mRNA translation when aerobic glycolysis is disengaged. Our data provide mechanistic insight to metabolic contribution to effector T cell function and suggest that T cell function may be finely tuned through modulation of glycolytic activity.

In Brief

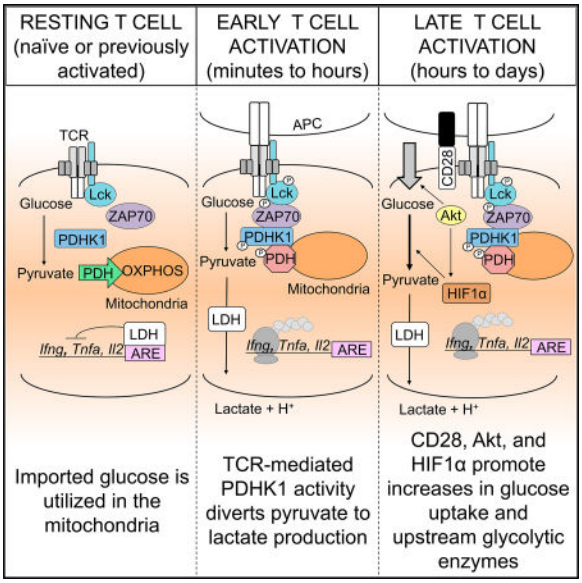

Menk et al. show rapid induction of aerobic glycolysis after activation of effector T cells that is required for acute cytokine production. These data provide mechanistic insight into the regulation of T cell function through nutrient availability.

INTRODUCTION

The activation of T cells to proliferate and develop into armed, effector cells is a highly regulated process that relies on the balance of multiple signals. T cell receptor (TCR) ligation triggers tyrosine kinase signaling, and costimulatory signals like CD28 can amplify these signals and engage important serine and threonine kinase cascades such as Akt and mTOR, leading to full T cell activation and proliferation (Powell and Delgoffe, 2010). Metabolic and nutrient sensing pathways also play a crucial role in T cell fate (Pearce et al., 2013). Effector phase T cells perform aerobic glycolysis, a metabolic state also adopted by rapidly dividing cells like cancer cells, in which despite the presence of oxygen, glucose is fermented into lactate rather than oxidized in the mitochondria (Kim and Dang, 2006). Glycolysis rapidly keeps up with ATP demands in glucose-rich conditions (Pfeiffer et al., 2001), regenerates NAD^+, and preserves the biosynthetic nature of the mitochondria to generate material to support proliferation (Delgoffe and Powell, 2015). However, aerobic glycolysis likely not only supports cellular function energetically but also interfaces with the acquisition of effector function through differentiation (Peng et al., 2016) and support of cytokine synthesis (Chang et al., 2013).

The molecular mechanism of the initiation of aerobic glycolysis in T cells and other cell types has been elusive (Palmer et al., 2015). Most of the glycolytic machinery is present in cells at baseline, although some proteins have isoforms that promote fermentative or oxidative pathways (pyruvate kinase M1 versus M2 and lactate dehydrogenase a versus b), suggesting that some transcriptional or post-transcriptional control might promote aerobic glycolysis (Palmer et al., 2015). Akt-mTOR signaling can also promote glycolysis through various mechanisms. Akt can phosphorylate GLUT1, facilitating its trafficking to the cell surface (Jacobs et al., 2008; Wieman et al., 2007); modify glycolytic enzymes like hexokinase; and transcriptionally regulate metabolism through modulation of transcription factors (Eijkelenboom and Burgering, 2013). mTOR can promote glycolysis through activation of hypoxia-inducible factor 1α (HIF1α), as well as Myc (Pollizzi and Powell, 2014). Yet it remains unclear whether initiation or commitment to glycolytic metabolism is an early, post-translationally regulated event or a late, transcriptionally programmed process.

Thus, we sought to dissect signaling events that initiate aerobic glycolysis in T cells and understand whether the kinetics of its initiation might provide insight into molecular determinants for these events. We also wanted to determine which T cell effector functions may be under the influence of rapid glycolysis induced by T cell activation and how the glycolytic machinery might directly interact with these pathways. We found that TCR activation initiates a signaling event that allows T cells to immediately perform aerobic glycolysis. This rapid activation-induced glycolysis is directly linked to T cell effector function, allowing T cells to initiate effector responses shortly after activation.

RESULTS

T Cell Activation Rapidly Induces Aerobic Glycolysis

To determine the glycolytic capacity of T cells in real time, we employed extracellular flux analysis using a Seahorse XFe96 bioanalyzer. Using both naive and previously activated, rested (PA-R) $CD4^+$ and $CD8^+$ T cells, T cells were activated for 6 hr *in vitro* with plate-bound anti-CD3 and anti-CD28, and oxidative metabolism (oxygen consumption rate [OCR]) and glycolysis (extracellular acidification rate [ECAR]) were measured. Consistent with previous findings, PA-R and naive T cells switch metabolic states within 6 hr of activation (Figures 1A and 1B) (van der Windt et al., 2013).

To identify when during this 6-hr period glycolysis may be activated, naive $CD8^+$ T cells were equilibrated in the Seahorse instrument for 30 min, and streptavidin-complexed anti-CD3 and anti-CD28 were injected to crosslink the TCR and ligate CD28. T cells engaged glycolysis within minutes of TCR activation, reaching a peak within 15 min and remaining glycolytic for the duration of the assay (Figure 1C). A concomitant loss of oxidative phosphorylation slowly occurred, reaching equilibrium around 2 hr post-stimulation (Figure 1D). Oligomycin treatment, inhibiting mitochondrial ATP synthase and stimulating cells to perform maximal levels of glycolysis, revealed that TCR ligation immediately and effectively engaged the entire glycolytic reserve of both PA-R and naive T cells (Figures 1E and 1F). ECAR activity correlated to increases in extracellular lactate concentration at time points consistent with this early change (Figures 1G and 1H). Thus, T cell activation induces

a major metabolic change in the cell, the stimulation of nearly all capable aerobic glycolysis, within minutes.

TCR Signaling Alone Can Mediate Rapid Activation-Induced Glycolysis

CD28 signaling can sustain glycolysis partly through the activation of phosphatidylinositol 3-kinase (PI3K)-Akt signaling (Frauwirth et al., 2002; Jacobs et al., 2008; Zheng et al., 2009). However, CD28 signaling was dispensable for the rapid initiation of aerobic glycolysis in both freshly isolated and PA-R $CD8^+$ T cells (Figure 2A; Figure S1A). TCR signal strength determined the magnitude of glycolytic switching that occurred (Figure 2B; Figure S1B). Although CD28 has been shown to act as a signal amplifier for TCR-mediated signals, neither PA-R nor naive T cells showed enhancement of rapid activation-induced glycolysis when CD28 was combined with suboptimal TCR stimulation (Figure 2B; Figure S1B), potentially because $CD8^+$ effector T cells are often considered costimulation independent (Flynn and Müllbacher, 1996). Stimulating naive T cells in hours-long culture revealed that although the initial switch to glycolysis was independent of CD28 signaling (Figures 2A and 2B), sustained glycolytic function required CD28 signaling (Figure 2C), Thus, although CD28 signaling may be required for initiating transcriptional or translational changes in cellular metabolism, it is dispensable for the initiation of glycolysis that occurs just after TCR engagement.

Rapid Activation-Induced Glycolysis Is Mediated by PDHK1 in a Manner Independent of Transcription, Translation, and Glucose Flux

To examine the nature of this TCR-induced glycolysis, T cells were treated with actinomycin D or cycloheximide before activation, showing that neither new transcription nor translation was necessary to initiate rapid glycolysis (Figure 3A). Furthermore, fluorescent 2-NBD-glucose uptake analysis showed glucose uptake was not elevated during these activation time points, occurring only late after stimulation (24 hr) (Figure 3B). Given that many enzymes in the glycolytic pathway can be post-translationally modified, TCR-induced changes in glycolytic enzyme phosphorylation upon T cell activation were measured, showing no changes in phosphorylation of previously reported modified enzymes in the glycolytic pathway, including hexokinase, phosphoglycerasemutase, enolase, pyruvate kinase, or lactate dehydrogenase (LDH) (Figures S2A and S2B). This does not rule out other methods of modulation of glycolytic enzyme activity, but because TCR activation is driven by phosphorylation, its contribution is likely through this mechanism. These results suggested that the extracellular acidification observed immediately after T cell activation was not due to changes in glucose uptake or increases in glycolytic flux but rather due to changes in glucose processing.

Pyruvate flux into mitochondria is controlled by pyruvate dehydrogenase (PDH), which both facilitates pyruvate import into the mitochondria and catalyzes its conversion to acetyl-coenzyme A (CoA) for the tricarboxylic acid (TCA) cycle (Patel et al., 2014). A prominent form of PDH regulation is modification by phosphorylation by the glycolytic gatekeeper pyruvate dehydrogenase kinase 1 (PDHK1, encoded by *Pdk1*) (Patel et al., 2014), resulting in inhibition of PDH function, blocking pyruvate flow into mitochondria, and facilitating lactic acid conversion by LDH. In cancer, PDHK1 can be phosphorylated by oncogenic

tyrosine kinases, stimulating its function to promote glycolysis (Hitosugi et al., 2011). Tyrosine phosphorylation of PDHK1 (measured using a phosphotyrosine immunoprecipitation and immunoblotting, and a specific phosphotyrosine antibody in whole-cell lysates) was rapidly induced upon TCR ligation and in a CD28-independent manner in T cells (Figure 3C; Figure S2C). We employed dichloroacetate (DCA), a specific inhibitor of PDHK1, to block activity of PDHK1 in the presence of TCR signals (Jha and Suk, 2013; Kankotia and Stacpoole, 2014; Michelakis et al., 2008). Inhibition of PDHK1 with DCA prevented the initiation of glycolysis in PA-R T cells, shown both using Seahorse ECAR and direct lactate measurements (Figures 3D and 3E). The activity of PDHK1, read out by its phosphorylation of PDH, was also increased upon T cell activation and inhibited by DCA treatment (Figure S2D). Furthermore, DCA treatment of T cells already undergoing rapid activation-induced glycolysis reduced ECAR to preactivation levels (Figure 3F).

To support the hypothesis that activation-induced PDHK1 activity alters the path of glucose processing, freshly isolated T cells were stimulated with anti-CD3 alone in normal glucose containing media for 30 min and then pulsed with uniformly labeled ^{13}C-glucose for another 30 min to conduct isotopic flux analysis (Figure S2E). Glucose-derived pyruvate levels were unchanged at 30 min between resting and stimulated cells, confirming prior notions that glycolytic enzymatic activity that produces pyruvate from glucose was not altered by TCR activation (Figure S2F). ^{13}C-labeled lactate was markedly increased in the media in response to TCR signaling in a DCA-dependent manner (and thus PDHK1-dependent manner) (Figure S2G). Finally, consistent with the notion that PDHK1 activation inhibits pyruvate processing in the mitochondria, less incorporation of labeled carbon was observed in the TCA cycle intermediates malate and citrate in response to stimulation, which was mitigated by DCA treatment (Figures S2H and S2I). However, only glucose-derived TCA cycle activity was inhibited, because the abundance of unlabeled TCA cycle intermediates remained unchanged regardless of treatment (Figure S2J).

Genetic targeting of PDHK1 was also employed to determine its role in glycolytic switching. PDHK1 was knocked down using retroviral RNA interference during CD8$^+$ T cell expansion (Figure 3G), revealing a significant decrease in activation-induced glycolysis (Figure 3H). Thus, PDHK1 is an important signaling node induced by early T cell activation that facilitates the rapid switch in the bioenergetic fate of glucose.

The Glycolytic Gatekeeper PDHK1 Is Activated by Early TCR Signaling

TCR engagement induces tyrosine phosphorylation of several kinases, and previous studies have suggested that, in cancer, oncogenic receptor tyrosine kinases (RTKs) bind to and phosphorylate PDHK1, especially FGFR1 (Hitosugi et al., 2011). Two TCR-induced kinases, ZAP-70 and Lck share significant homology with FGFR1, suggesting these might bind to PDHK1. PDHK1 was coimmunoprecipitated with Lck at steady state, and upon activation, PDHK1 bound ZAP-70 suggesting these proteins might exist in a complex (Figure 4A). ZAP-70-deficient Jurkat T cells failed to engage rapid glycolysis upon stimulation with OKT3 (Figures S3A and S3B). To determine to which early TCR signaling molecules PDHK1 directly interacted with upon T cell activation, HEK293T cells were transfected with different combinations of PDHK1, linker of activated T cells (LAT), and

constitutively active Lck or Zap70 to study their interactions in a non-T cell system (Levin et al., 2008). PDHK1 could bind directly to Lck or Lat, but interaction with Zap70 required the presence of Lck or Lat (Figure 4B). Total internal reflection fluorescence (TIRF) microscopy of PA-R T cells on stimulatory lipid bilayers revealed that that total and phosphorylated PDHK1 were present at and were significantly associated with the T cell synapse upon T cell activation (Figure 4C).

To determine whether more distal signaling pathways were engaging the glycolytic machinery, T cells were treated with the minimal effective doses of several reported signaling module inhibitors induced during TCR activation, confirming Lck inhibition prevented PDHK1 phosphorylation and rapid activation-induced glycolysis (Figures 4D and 4E) and preventing the interaction of PDHK1 and Zap70 (Figure 4F). In stark contrast, Akt, mTOR, ERK, PI3K, PLC, protein kinase C (PKC), and calcium flux were dispensable for induction of rapid glycolysis and phosphorylation of PDHK1 (Figures 4D and 4E; Figure S3C). These results were particularly surprising because Akt has been implicated in early-immediate glycolysis in human memory T cells (Gubser et al., 2013). PI3K-Akt was also not sufficient to induce glycolysis, because in-Seahorse stimulation of PI3K with a PTEN inhibitor did not engage glycolysis (Figure S3D). Likewise, T cells from *Rictor*$^{f/f}$*Cd4*^{Cre} mice, in which Akt cannot be phosphorylated by mTORC2 (Pollizzi et al., 2015), were still able to initiate glycolysis after activation (Figure S3E).

Another previously reported contributor to glycolysis is HIF1α, which promotes glycolysis through transcriptional and post-translational changes, including the upregulation of PDHK1 (Lee and Simon, 2012). Naive T cells from *Hif1a*$^{f/f}$*Cd4*^{Cre} mice were able to initiate rapid glycolysis, as well as their wild-type counterparts (Figure S3F). Activation and expansion of HIF1α-deficient T cells revealed their basal glycolysis was lower than that of wild-type cells, consistent with the notion that HIF1α promotes a transcriptional glycolytic program (Figure S3G). However, these previously activated HIF1α-deficient T cells induce rapid glycolysis upon reactivation to the same degree relative to their basal levels, indicating that PDHK1's role in glycolysis is distinct from that of HIF1α (Figures S3G and S3H). Hyperactivation of PKC alone using the phorbol ester phorbol 12-myristate 13-acetate (PMA) can also initiate glycolysis in PA-R T cells, but to a lesser degree, with distinct kinetics and without engaging PDHK1 (Figures S3I and S3J). Thus, the initiation of glycolysis occurs directly downstream of the TCR in an Lck-dependent manner via the kinase PDHK1.

Rapid Activation-Induced Glycolysis Regulates Distinct Acute Effector Functions

Aerobic glycolysis has been previously shown to be critical for T cell effector function, as measured by cytokine production, but used interchangeably with oxidative phosphorylation (OXPHOS) to meet the metabolic needs of T cell proliferation and expansion (Chang et al., 2013; Palmer et al., 2015). Consistent with these reports, at high doses, DCA-mediated PDHK1 inhibition had effects on proliferation after 96 hr (Figure S4A). Because this pathway is induced minutes after activation, its major importance may be to support the early-immediate, rapid effector function of T cells competent to produce cytokines.

Previous reports have suggested glycolysis is important for the synthesis of cytokine intypical stimulation conditions (Chang et al., 2013). Inhibition of PDHK1 in the early phase inhibited the ability of effector $CD8^+$ T cells to rapidly synthesize interferon gamma (IFNγ), interleukin (IL)-2, or tumor necrosis factor alpha (TNFα) early after TCR activation (1 hr–6 hr) (Figures 5A and B).DCA treatment also inhibited cytokine production in overnight activation, suggesting that although this switch is induced quickly upon activation, it is used later into the activation phase to facilitate cytokine synthesis and secretion (Figure 5C). To fully interrogate effector function, the cytotoxic potential of T cells was also examined. Inhibition of PDHK1-mediated glycolysis had a minimal effect on cytolytic capacity (Figure 5D), and DCA-treated cells were still able to produce the cytolytic molecules perforin and granzyme B (Figure S4B). PDHK1 inhibition by DCA was not toxic to the cells (Figure S4C). Consistent with the role of PDHK1 as a gatekeeper enzyme rather than a promoter of glycolytic flux, PDHK1 inhibition did not change the ability of T cells to take up glucose (Figure S4D). PDHK1 inhibition had similar effects on *in vivo*-generated $CD8^+$ effector T cells, using OT-I transfer and ovalbumin (OVA)-expressing *Vaccinia* virus: inhibition of cytokine production (Figure S4E) and preserved cytotoxic function *in vivo* (Figure 5E).

Although we and others have shown that aerobic glycolysis promotes acute effector function of T cells, there have been reports that aerobic glycolysis also promotes IFNγ competency during Th1 differentiation through a long-term, epigenetic mechanism (Peng et al., 2016). These studies were done with LDH-deficient animals, which have essentially irreversible inhibition of aerobic glycolysis. Employing pharmacological and reversible inhibition of aerobic glycolysis via DCA could thus both confirm the role of aerobic glycolysis in T cell differentiation and reveal a role for this pathway in acute effector function of T cells. Similar to previous reports using LDH-deficient T cells, inhibiting glycolysis for 7 days using the PDHK1 inhibitor DCA during PA-R T cell generation prevented T cell differentiation, as evidenced by an inability to produce IFNγ (Figure S4F). In addition, genetic targeting using retroviral RNA interference caused a decrease in cytokine production but had no effect on perforin or granzyme B production or the ability for the cells to kill their targets *in vitro* (Figures S4G–S4I). However, this inhibited cytokine synthesis occurred even when PDHK1 was active during the restimulation (DCA treatment during differentiation but washed out before restimulation) (Figure S4F). This suggests that aerobic glycolysis plays a secondary, long-term role in maintaining the T cell differentiation state in a manner distinct from the control of acute cytokine production we and others have observed.

Our previous data suggested that naive T cells also engaged this rapid glycolytic switch in response to TCR stimulation (Figures 1 and 2). Because naive T cells generally are not cytokine competent, we explored the contribution of this early glycolytic switch to their function, taking advantage of the reversibility of DCA-mediated PDHK1 inhibition. Washout experiments, in which DCA was only present during 12 hr of initial stimulation, revealed that this early glycolytic switch was dispensable for expansion of naive T cells, suggesting that its contribution might be limited to the acute phase (Figure S5A). In addition, when PDHK1 was inhibited only during activation, it did not negatively affect glucose uptake, mitochondrial mass or polarization, or the ability for T cells to produce IFNγ after restimulation, suggesting that PDHK1-mediated glycolysis is especially important for short-term functions in response to acute activation (Figures S5B and S5C).

Although naive T cells do not synthesize cytokine, they rapidly make other chemical mediators, including chemokines like CCL3. Naive ($CD62L^{hi}CD44^{lo}$) OT-I T cells stimulated with peptide and antigen presenting cells (APCs) for 5 hr revealed CCL3 production was strikingly dependent on glycolysis (Figure S5D). Thus, it appears that this rapid metabolic change is important, both in naive and in PA-R effector T cells, in early, acute synthetic functions of T cells.

Rapid Activation-Induced Glycolysis Supports Post-transcriptional Control of Cytokine Synthesis through LDH

Although, as demonstrated earlier, aerobic glycolysis can contribute to effector function by promoting epigenetic changes supporting T cell differentiation, our data and others' also suggest a more immediate role for glycolysis in acute effector function. Although T cells undergo this major metabolic change during their early cytokine-producing phase, they do not increase their ability to take up glucose (Figure 3B). This suggested that the ability to engage aerobic glycolysis and thus support effector function would depend on the availability of glucose in the environment, acting as a sensor for nutrient availability. To test this, PA-R T cells were stimulated for a short time (3 hr) in the Seahorse in various suboptimal concentrations of glucose, revealing that the extent of PDHK1-mediated aerobic glycolysis depended on the availability of glucose, reaching saturation around 5 mM, after which no more glucose could be fermented (Figure 6A). Measurement of IFNγ secretion from these same Seahorse assay wells by ELISA revealed that cytokine production, while occurring in even zero-glucose conditions, showed a substantial increase as glucose availability increased (Figure 6B). This is in agreement with previous data suggesting cytokine synthesis was linked to extracellular glucose availability (Blagih et al., 2015). DCA treatment during the assay revealed that this supplemental cytokine synthesis depended on the PDHK1-mediated switch (Figure 6B). However, neither glucose concentrations nor PDHK1 activity appreciably changed the mRNA levels of *Ifng* (or *Tnf* or *Il2*) cytokine transcripts, even though these cells produce lower amounts of these proteins in either short-term (3 hr) or long-term (overnight) stimulations (Figures 6B and 6C; Figure S6). Studies have revealed a role for metabolic enzymes, especially GAPDH, in modulating cytokine mRNA stability (Chang et al., 2013). However, GAPDH, an enzyme several steps upstream of pyruvate, is used for glucose processing regardless of whether pyruvate is oxidized in mitochondria or fermented into lactate, and DCA treatment fails to inhibit GAPDH activity (Schmidt et al., 2011). However, LDH, which catalyzes the inter-conversion of pyruvate and lactate and is the only glycolytic enzyme with differential function in DCA-treated cells, has also been shown to have RNA-binding function. Previously studies have shown that it, like GAPDH, binds the AU-rich element (ARE) present in the 3′ UTR of mRNAs like granulocyte-macrophage colony stimulating factor (GM-CSF) and with greater affinity than GAPDH (Pioli et al., 2002). We activated PA-R $CD8^+$ T cells overnight in the presence or absence of DCA and performed RNA immunoprecipitation using anti-LDH antibodies (Figure 6D). LDH bound mRNA transcripts for the cytokines IFNγ, TNFα, and IL-2 in resting T cells, but upon activation, this binding was significantly reduced. Inhibition of PDHK1-mediated glycolysis during activation resulted in enhanced binding of LDH to cytokine mRNA, suggesting that LDH may be mediating post-transcriptional regulation of these cytokine transcripts (Figure 6D). LDH failed to bind transcripts for the cytotoxicity

gene *Gzmb*, which lacks an ARE in its 3′ UTR (Figure 6D), supporting the notion that cytolytic capacity does not require glycolysis (Figure 5E; Figures S4B, S4H, and S4I). These experiments were conducted using a full overnight stimulation to induce optimal transcription and translation of cytokine rather than using an acute activation protocol. However, the PDHK1-mediated glycolytic switch is important for optimal elaboration of cytokine even in overnight stimulatory conditions (Figure 5C). To confirm the role of the ARE in LDH-mediated mRNA control, T cells were assayed from mice in which the *Ifng* 3′ UTR has been replaced with a scrambled nucleotide insertion, resulting in transcript that is the same size as wild-type *Ifng* but lacks the ARE (Hodge et al., 2014). T cells with this mutation are resistant to DCA-mediated inhibition of IFNγ synthesis (Figures 6E and 6F). Specificity of this effect was confirmed, because IL-2 was still repressed with DCA treatment in $Ifng^{\Delta ARE}$ T cells (Figure 6F). Thus, the initiation of aerobic glycolysis in T cells promotes effector cytokine production partly through the alleviation of LDH-mediated repression of mRNA translation.

DISCUSSION

The immune response interfaces heavily with metabolic and nutrient sensing pathways, the study of which has garnered interest in recent years (Rathmell, 2012). Although it has been known for decades that lymphocytes carry out aerobic glycolysis during activation (Roos and Loos, 1973), it has only recently become clear which signals may initiate or sustain this metabolism. In addition, the functional relevance of aerobic glycolysis, in particular the epigenetic and post-transcriptional control of effector function, has just been realized (Chang et al., 2013; Peng et al., 2016; van der Windt et al., 2013). Our results reveal four previously unappreciated aspects of activation-mediated metabolic reprogramming.

First, our data suggest that rapid activation-induced glycolysis, occurring immediately after TCR ligation, bears hallmarks that make this metabolic pathway distinct from the aerobic glycolysis of actively proliferating T cells. It occurs in a transcription- and translation-independent manner and does not enhance or require increased glucose uptake in T cells. Rather, our studies support a model in which this rapid activation-induced glycolysis is a distinct metabolic switch promoting pyruvate to lactate conversion immediately after activation to support short-term effector function.

Second, although CD28 and Akt signaling have previously been shown to be critical for the upregulation of metabolic machinery and the maintenance of glycolysis throughout expansion (Frauwirth et al., 2002; Rathmell et al., 2003; Zheng et al., 2009), the initiating events of glycolysis, occurring almost immediately after T cell activation, are CD28 and Akt independent. Although Akt has been associated with rapid induction of glycolysis previously using effector memory cells (Gubser et al., 2013), our studies using the minimal inhibitory dose of Akt/PI3K inhibition, as well as genetic deletion of the Akt kinase, reveal this pathway is dispensable for this rapid-activation-induced glycolysis, at least in murine effector T cells. It is possible that Akt may be playing a larger role in bona fide memory T cells (rather than *in vitro*-generated PA-R T cells) to promote this metabolic switch, suggesting additional complexity in the regulation of these signaling pathways in distinct differentiation states.

Third, our studies suggest that PDHK1-mediated initiation of aerobic glycolysis, while required for optimal cytokine production and secretion (Chang et al., 2013), is dispensable for other effector functions, such as proliferation and cytolytic function. Our studies are in agreement with previously published data implicating glycolysis in the post-translational control of cytokine translation (Blagih et al., 2015; Chang et al., 2013) but reveal that cytotoxicity is an effector function that can be distinguished, metabolically, from cytokine production. Furthermore, using PDHK1 inhibition as a reversible inhibitor of LDH activity, we confirmed that aerobic glycolysis plays a role in regulation of differentiation in a manner that is distinct from its control of acute effector function. This was accomplished using DCA, which pharmacologically but reversibly inhibits PDHK1 activity. Although we confirmed the metabolic and functional roles of PDHK1 using RNA interference, the irreversibility of genetic deletion made separating acute functional versus epigenetic or differentiation effects difficult. Future directions will employ inducible genetic inhibition experiments to more specifically inhibit PDHK1's activity. PDHK1 activity has been previously reported in $CD4^+$ T helper cells as selectively important for PMA- and ionomycin-elicited IL-17 cytokine production (Gerriets et al., 2015). Our data in $CD8^+$ T cells are largely in agreement with this previous work, although by stimulating using TCR crosslinking (anti-CD3 and/or cognate peptide), we have revealed that additional cytokines (*Ifng, Il2*, and *Tnfa*) are under control of PDHK1-mediated aerobic glycolysis. In addition, by using *in vivo*-generated effector T cells using *Vaccinia* virus, we highlight the link between our *in vitro*-generated findings *in vivo* biological significance, although more elegant detection methods will surely enable future functional and metabolic analysis of acutely activated T cells in *in vivo* disease settings.

Fourth, our data support a role for LDH as a key node linking aerobic glycolysis and cytokine production. LDH, like GAPDH and other metabolic enzymes, binds AREs present in cytokine (and presumably chemokine) transcripts, repressing translation in a non-glycolytic state. Thus, part of the glycolytic phenotype is the relief of cytokine mRNA from LDH-mediated translational repression. Because key cytotoxic granule genes like *Gzmb* and *Prf1* lack an ARE in their 3′ UTR, they are not regulated by aerobic glycolysis, in concordance with our functional data. Our data in naive T cells show that CCL3, a chemokine rapidly secreted in response to activation, is also under glycolytic control: it too bears an ARE in its 3′ UTR (Kang et al., 2011), suggesting that a range of proteins may be modulated in response to rapid glycolysis. These data provide evidence that rapid activation-induced glycolysis is a general T cell phenomenon, regardless of differentiation state. It is the goal of future work to determine the full implication of these findings, such as other mRNA sequences regulated by glycolytic enzymes and differences in regulated mRNA between T cell types and differentiation states.

In agreement with previous reports (Chang et al., 2013), inhibition of aerobic glycolysis during short-term activation (30 min to 6 hr) does not repress cytokine production, resulting in a consistent 40%–50% reduction in cytokine levels. We believe is not a technical issue but rather indicative of real biology. This pathway, by its nature, does not increase glucose uptake or glycolytic processing; it changes how pyruvate is metabolized, thereby affecting the activity of LDH. Thus, our data support a model in which, during early T cell activation, glycolysis acts as a rheostat or throttle for cytokine production, tuning the amount of

cytokine translation to match the metabolic state of the microenvironment, which we confirmed in glucose titration experiments. This has wide-ranging implications for T cell activation in the tissues, which typically possess far lower concentrations of glucose than typical cell culture media. Of particular interest is activation in the tumor microenvironment, which has dramatically reduced concentrations of glucose and increased levels of lactic acid, which both may alter the ability of even optimally activated T cells to effectively synthesize cytokines (Ho et al., 2015; Scharping and Delgoffe, 2016). It is the goal of future work to translate these mechanistic insights, identifying how glycolytic activity and subsequent effector molecule synthesis may be modulated during *in vivo* activation, especially in environments in which nutrients may be limited or abundant.

Many other cell types demonstrate rapid effector functions, synthesizing cytokines hours after activation, which may be regulated by this rapid activation-induced glycolysis. In support of this, we have shown that mast cells stimulated through the FcεR rapidly trigger glycolysis that is important for their cytokine production (Phong et al., 2017). We anticipate other rapid cytokine-producing cells will use similar tyrosine signaling cascades to promote rapid glycolysis, including FcγR-stimulated natural killer (NK) cells, invariant natural killer T (iNKT) cells, and B cells.

Previous studies have implicated glycolysis in T cell activation, avoidance of anergy, and the bias of effector versus memory differentiation (Frauwirth et al., 2002; Gubser et al., 2013; Jacobs et al., 2008; Sukumar et al., 2013; van der Windt et al., 2013; Zheng et al., 2009). Many studies use 2-deoxy-d-glucose (2DG), which inhibits the entire glycolytic pathway starting at hexokinase, as well as N-linked glycosylation (Zhang et al., 2014). Other studies have use galactose, which through the Leloir pathway can still enter the glycolytic process (Bustamante and Pedersen, 1977). In addition, some studies have used steady-state genetic perturbations many of these enzymes (Peng et al., 2016). Inhibition of PDHK1, in contrast, does not perturb glucose flux or enzymatically perturb any stage of glycolysis, which effectively targets only the activation-induced glycolytic pathways (Zhang et al., 2015). Furthermore, we believe that using pharmacological, reversible inhibition of this switch rather than genetic deletion has confirmed the role of this pathway in epigenetic control of differentiation, as well as acute control of effector function.

Our data support a model placing these early, key changes in glucose metabolism central to the execution of the acute effector T cell program in differentiated, cytokine competent cells, as well as early synthesis programs like chemokine production even in naive T cells. This is initiated by the TCR at the level of PDHK1 and is functionally modulatory at the level of LDH. This antigen receptor-mediated, rapid activation-induced glycolysis constitutes a metabolic pathway that is fundamentally distinct from those longer-term, transcriptionally regulated changes that characterize proliferating T cells. Our work also suggests that different functions of lymphocytes may be effectively distinguished through metabolic means. As such, understanding how these distinct metabolic pathways interface with immune effector programs may allow for the use of metabolic intervention to functionally modulate the immune response with greater precision.

EXPERIMENTAL PROCEDURES

Mice

All animal work was done in accordance with the Institutional Animal Care and Use Committee of the University of Pittsburgh. All mice were housed in specific pathogen-free conditions before use. Both male and female mice were used, and mice were 6–8 weeks old at time of use. C57BL/6, OT-I, *Cd4*^{Cre}, and *Hif1a*$^{f/f}$ mice were obtained from The Jackson Laboratory. Mice lacking the ARE of *Ifng* were generated by Dr. Howard Young (National Cancer Institute [NCI]). *Rictor*$^{f/f}$*Cd4*^{cre} and littermate controls were obtained from Dr. Jonathan Powell (Johns Hopkins University).

T Cell Isolations

Spleen and lymph node CD4$^+$ and CD8$^+$ T cells were magnetically isolated from 6- to 8-week-old mice as previously described (Scharping et al., 2016). Naive T cells were isolated using CD44 (IM7)-biotin-activated magnetic depletion or by flow cytometric sorting (CD8$^+$ or CD4$^+$ CD62L^{hi}CD44^{lo}) on a Beckman Coulter Mo-Flo Astrios High Speed Cell Sorter.

PA-R T Cell Generation

To generate PA-R T cells, CD4$^+$ or CD8$^+$ T cells were freshly isolated from C57BL/6 and stimulated at 10 × 10^6/mL in complete RPMI with plate-bound anti-CD3 (3 μg/mL, BD Biosciences) and anti-CD28 (2 μg/mL, BD Biosciences), or spleen or node preparations harvested from OT-I mice were stimulated with 250 ng/mL SIINFEKL peptide (AnaSpec) in the presence of 50 U/mL IL-2 (PeproTech) for 24 hr. Cells were then expanded into complete RPMI supplemented with 50 U/mL IL-2 for 1 day, 25 U/mL IL-2 for an additional 4 days, and then 10 U/mL IL-2 for an additional 1–2 days. Some were also cultured with DCA (CAS 2156-56-1) (Fisher). *Vaccinia*-OVA, generated by J.R. Bennink (Bacik et al., 1994) and provided by Dr. Jonathan Powell (Johns Hopkins University), was used as previously described to generate previously activated cells *in vivo* (Scharping et al., 2016).

Metabolic Assays

Naive or PA-R T cells were plated on Cell-Tak-coated Seahorse Bioanalyzer XFe96 culture plates (300,000 or 100,000 cells/well, respectively) in assay media consisting of minimal, unbuffered DMEM supplemented with 1% BSA and 25 mM glucose, 2 mM glutamine, and for some experiments, 1 mM sodium pyruvate. Basal rates were taken for 30 min, and then streptavidin-complexed anti-CD3^{bio} at 3 μg/mL ± anti-CD28 at 2 μg/mL or PMA (CAS 16561-29-8) (Fisher) was injected and readings continued for 1–6 hr. In some experiments, oligomycin (2 μM), carbonyl cyanide p-trifluoromethoxyphenylhydrazone (FCCP) (0.5 μM), 2-deoxy-d-glucose (10 mM) rotenone/antimycin A (0.5 μM), and DCA (20 mM) were injected to obtain maximal respiratory and control values. Inhibitors used for some experiments include 5–50 mM DCA, 10 nM Lck inhibitor RK24466 (CAS 213743-31-8), 500 nM Akt inhibitor VIII (CAS 612847-09-3), 500 nM rapamycin (CAS 53123-88-9) (Cayman Chemical), 10 μM ERK inhibitor U0126 (CAS 109511-58-2), 10 μM PI3K inhibitor LY294002 (CAS 154447-36-6), 100 nM PKC inhibitor sotratorin (CAS 425637-18-9), EDTA (CAS 67526-95-8), actinomycin D (CAS 50-76-0), cycloheximide

(CAS 66-81-9) (Cayman Chemical), 500 nM U-73122 PLCγ inhibitor (CAS 112648-68-7) (Sigma), and EGTA (CAS 67-42-5) (Fisher). For Jurkat T cell experiments, wild-type (WT) or ZAP-70-deficient cells were stimulated with OKT3 (BioLegend) complexed using anti-mouse immunoglobulin G (IgG). Because ECAR values tend to vary among experiments, most figure panels have both a representative trace and normalized data (calculated as the difference between maximal and basal ECAR values). Lactate was measured using the colorimetric kit from Abcam.

Retroviral RNA Interference

Short hairpin RNA (shRNA) retroviral constructs were purchased from OriGene, and OT-I T cells were transduced as previously described (Scharping et al., 2016), except that puromycin (2 μg/mL) was used for selection.

Immunoblotting and Immunoprecipitation Analysis

Immunoblotting was performed as previously described (Delgoffe et al., 2009). Naive or PA-R T cells were stimulated with anti-$CD3^{bio}$ at 3 μg/mL complexed with streptavidin at 1.5 μg/mL (AnaSpec) for various times in the presence or absence of anti-CD28 at 2 μg/mL or with PMA. HEK293T cells transfected with combinations of Lck, LAT, ZAP-70, or PDHK1 overexpression vectors (A. Weiss) were used (no stimulation). All antibodies for IP or immunoblots (IBs) were obtained from Cell Signaling Technology except pPDH (S293) from Novus Biologicals and β-actin from Santa Cruz Biotechnology. IBs were detected via standard secondary detection and chemiluminescent exposure to film. Digitally captured films were analyzed densitometrically by ImageJ software.

Microscopy

Immunological synapse formation was analyzed in response to lipid bilayer stimulation as previously described (Guy et al., 2013). Briefly, lipid bilayers containing ICAM-1 and Alexa Fluor (AF)647-labeled anti-TCR antibodies were prepared. Resting OT-I $CD8^+$ T cells were stimulated for 30 min before fixation with 4% paraformaldehyde, permeabilization with 0.1% T-100, and staining with antibodies overnight at 4°C. AF568-conjugated secondary antibodies and AF488-conjugated phalloidin (Fisher) were applied for 1 hr before analysis using TIRF microscopy. Images were acquired using an inverted TiE Nikon microscope equipped with a 100× 1.45 numerical aperture (NA) oil objective, motorized TIRF illumination, Andor DU-897 high-speed electron-multiplying charge-coupled device (EMCCD) camera, and Agilent laser launch. Analysis of fluorescent intensities for each channel were determined for individual pixels using Nikon Elements software.

Functional Readouts

Cytokine production and proliferation were assessed as previously described (Scharping et al., 2016), with some minor changes. $CD8^+$ T cells were stimulated with 1 to 3 μg/mL plate-bound anti-CD3 and 2 μg/mL soluble anti-CD28 (for C57BL/6 T cells) or 250 ng/mL SIINFEKL peptide + antigen-presenting cells (for OT-I T cells) for 3–24 hr (final 4 hr in the presence of brefeldin A) and then stained intracellularly for cytokines, or secreted IFNγ was measured using an ELISA assay. For naive T cell functional assays, $CD62L^{hi}CD44^{lo}$ OT-I T

cells were purified flow cytometrically, stimulated for 5 hr with T cell-depleted splenocytes and SIINFEKL peptide in the presence of brefeldin A, and then stained intracellularly for CCL3 (BioLegend). *In vitro* cytotoxicity was assessed as previously described (Scharping et al., 2017). *In vivo* cytotoxicity was measured as the change in the ratio of carboxyfluorescein succinimidyl ester $(CFSE)^{hi}$ (OVA peptide loaded) to $CFSE^{lo}$ (irrelevant control) cells after adoptive transfer of OT-I T cells and differentially CFSE-labeled target cells relative to naive mice.

RNA Immunoprecipitation

PA-R T cells were activated 18 hr with plate-bound anti-CD3 at 3 μg/mL and anti-CD28 at 2 μg/mL in the presence or absence of DCA. Cells were harvested and crosslinked with 1% formaldehyde 10 min at room temperature (RT). Cells were then lysed in RNA immunoprecipitation (RIP) lysis buffer (150 mM KCl, 25 mM Tris, 1 mM EDTA, 1% NP-40) and precleared. Lysates were then incubated with 2 μg of anti-LDH A (LDHA) or its species-matched isotype control (Santa Cruz Biotechnology), rotating overnight at 4°C, followed by addition of 25 μL of protein A/G agarose. Beads were washed five times in RIP lysis buffer before elution with 1% SDS and 100 mM $NaHCO_3$. Crosslinks were reversed with NaCl for 5 hr at 65°C before Trizol RNA extraction and cDNA generation.

Statistical Analysis

The p values were calculated using an unpaired Student's t test or Pearson's correlation. Values of $p < 0.05$ were considered significant. Values of $p < 0.05$ were ranked as $*p < 0.05$, $**p < 0.01$, $***p < 0.001$, and $****p < 0.0001$.

Supplementary Material

Refer to Web version on PubMed Central for supplementary material.

Acknowledgments

The authors thank C.H. Patel and J.D. Powell for rictor-deficient T cells and *Vaccinia*-OVA, L.P. Kane for ZAP-70-deficient P116 and P116.cl39 Jurkat T cells, B. Au-Yeong and A. Weiss for TCR signaling overexpression constructs, and D.A.A. Vignali, L.P. Kane, R.L. Ferris, and M.J. Shlomchik for critical reading of this manuscript. This work was supported by the Sidney Kimmel Foundation for Cancer Research Scholar Award (SKF-015-039), a Stand Up 2 Cancer-American Association of Cancer Research Innovative Research Grant (SU2C-AACR-IRG-04-16), the NIH Director's New Innovator Award (DP2AI136598), start-up funds (to G.M.D.) through the Tumor Microenvironment Center at the University of Pittsburgh, and the National Cancer Institute (T32 CA082084 and F99CA222711 to N.E.S). The work was also supported in part by the intramural research program of the National Cancer Institute (to H.A.Y.). This project used the UPMC Hillman Cancer Center Animal Facility and Cytometry Facility, which are supported in part by award P30CA047904.

References

Bacik I, Cox JH, Anderson R, Yewdell JW, Bennink JR. TAP (transporter associated with antigen processing)-independent presentation of endogenously synthesized peptides is enhanced by endoplasmic reticulum insertion sequences located at the amino- but not carboxyl-terminus of the peptide. J. Immunol. 1994; 152:381–387. [PubMed: 8283027]

Blagih J, Coulombe F, Vincent EE, Dupuy F, Galicia-Vázquez G, Yurchenko E, Raissi TC, van der Windt GJ, Viollet B, Pearce EL, et al. The energy sensor AMPK regulates T cell metabolic adaptation and effector responses in vivo. Immunity. 2015; 42:41–54. [PubMed: 25607458]

Bustamante E, Pedersen PL. High aerobic glycolysis of rat hepatoma cells in culture: role of mitochondrial hexokinase. Proc. Natl. Acad. Sci. USA. 1977; 74:3735–3739. [PubMed: 198801]

Chang CH, Curtis JD, Maggi LB Jr, Faubert B, Villarino AV, O'Sullivan D, Huang SC, van der Windt GJ, Blagih J, Qiu J, et al. Posttranscriptional control of T cell effector function by aerobic glycolysis. Cell. 2013; 153:1239–1251. [PubMed: 23746840]

Delgoffe GM, Powell JD. Sugar, fat, and protein: new insights into what T cells crave. Curr. Opin. Immunol. 2015; 33:49–54. [PubMed: 25665466]

Delgoffe GM, Kole TP, Cotter RJ, Powell JD. Enhanced interaction between Hsp90 and raptor regulates mTOR signaling upon T cell activation. Mol. Immunol. 2009; 46:2694–2698. [PubMed: 19586661]

Eijkelenboom A, Burgering BM. FOXOs: signalling integrators for homeostasis maintenance. Nat. Rev. Mol. Cell Biol. 2013; 14:83–97. [PubMed: 23325358]

Flynn K, Müllbacher A. Memory alloreactive cytotoxic T cells do not require costimulation for activation *in vitro*. Immunol. Cell Biol. 1996; 74:413–420. [PubMed: 8912004]

Frauwirth KA, Riley JL, Harris MH, Parry RV, Rathmell JC, Plas DR, Elstrom RL, June CH, Thompson CB. The CD28 signaling pathway regulates glucose metabolism. Immunity. 2002; 16:769–777. [PubMed: 12121659]

Gerriets VA, Kishton RJ, Nichols AG, Macintyre AN, Inoue M, Ilkayeva O, Winter PS, Liu X, Priyadharshini B, Slawinska ME, et al. Metabolic programming and PDHK1 control CD4+ T cell subsets and inflammation. J. Clin. Invest. 2015; 125:194–207. [PubMed: 25437876]

Gubser PM, Bantug GR, Razik L, Fischer M, Dimeloe S, Hoenger G, Durovic B, Jauch A, Hess C. Rapid effector function of memory CD8+ T cells requires an immediate-early glycolytic switch. Nat. Immunol. 2013; 14:1064–1072. [PubMed: 23955661]

Guy CS, Vignali KM, Temirov J, Bettini ML, Overacre AE, Smeltzer M, Zhang H, Huppa JB, Tsai YH, Lobry C, et al. Distinct TCR signaling pathways drive proliferation and cytokine production in T cells. Nat. Immunol. 2013; 14:262–270. [PubMed: 23377202]

Hitosugi T, Fan J, Chung TW, Lythgoe K, Wang X, Xie J, Ge Q, Gu TL, Polakiewicz RD, Roesel JL, et al. Tyrosine phosphorylation of mitochondrial pyruvate dehydrogenase kinase 1 is important for cancer metabolism. Mol. Cell. 2011; 44:864–877. [PubMed: 22195962]

Ho PC, Bihuniak JD, Macintyre AN, Staron M, Liu X, Amezquita R, Tsui YC, Cui G, Micevic G, Perales JC, et al. Phosphoenolpyruvate is a metabolic checkpoint of anti-tumor T cell responses. Cell. 2015; 162:1217–1228. [PubMed: 26321681]

Hodge DL, Berthet C, Coppola V, Kastenmüller W, Buschman MD, Schaughency PM, Shirota H, Scarzello AJ, Subleski JJ, Anver MR, et al. IFN-gamma AU-rich element removal promotes chronic IFN-gamma expression and autoimmunity in mice. J. Autoimmun. 2014; 53:33–45. [PubMed: 24583068]

Jacobs SR, Herman CE, Maciver NJ, Wofford JA, Wieman HL, Hammen JJ, Rathmell JC. Glucose uptake is limiting in T cell activation and requires CD28-mediated Akt-dependent and independent pathways. J. Immunol. 2008; 180:4476–4486. [PubMed: 18354169]

Jha MK, Suk K. Pyruvate dehydrogenase kinase as a potential therapeutic target for malignant gliomas. Brain Tumor Res. Treat. 2013; 1:57–63. [PubMed: 24904893]

Kang JG, Amar MJ, Remaley AT, Kwon J, Blackshear PJ, Wang PY, Hwang PM. Zinc finger protein TTP interacts with CCL3 mRNA and regulates tissue inflammation. J. Immunol. 2011; 187:2696–2701. [PubMed: 21784977]

Kankotia S, Stacpoole PW. Dichloroacetate and cancer: new home for an orphan drug? Biochim. Biophys. Acta. 2014; 1846:617–629. [PubMed: 25157892]

Kim JW, Dang CV. Cancer's molecular sweet tooth and the Warburg effect. Cancer Res. 2006; 66:8927–8930. [PubMed: 16982728]

Lee KE, Simon MC. From stem cells to cancer stem cells: HIF takes the stage. Curr. Opin. Cell Biol. 2012; 24:232–235. [PubMed: 22296771]

Levin SE, Zhang C, Kadlecek TA, Shokat KM, Weiss A. Inhibition of ZAP-70 kinase activity via an analog-sensitive allele blocks T cell receptor and CD28 superagonist signaling. J. Biol. Chem. 2008; 283:15419–15430. [PubMed: 18378687]

Michelakis ED, Webster L, Mackey JR. Dichloroacetate (DCA) as a potential metabolic-targeting therapy for cancer. Br. J. Cancer. 2008; 99:989–994. [PubMed: 18766181]

Palmer CS, Ostrowski M, Balderson B, Christian N, Crowe SM. Glucose metabolism regulates T cell activation, differentiation, and functions. Front. Immunol. 2015; 6:1. [PubMed: 25657648]

Patel MS, Nemeria NS, Furey W, Jordan F. The pyruvate dehydrogenase complexes: structure-based function and regulation. J. Biol. Chem. 2014; 289:16615–16623. [PubMed: 24798336]

Pearce EL, Poffenberger MC, Chang CH, Jones RG. Fueling immunity: insights into metabolism and lymphocyte function. Science. 2013; 342:1242454. [PubMed: 24115444]

Peng M, Yin N, Chhangawala S, Xu K, Leslie CS, Li MO. Aerobic glycolysis promotes T helper 1 cell differentiation through an epigenetic mechanism. Science. 2016; 354:481–484. [PubMed: 27708054]

Pfeiffer T, Schuster S, Bonhoeffer S. Cooperation and competition in the evolution of ATP-producing pathways. Science. 2001; 292:504–507. [PubMed: 11283355]

Phong B, Avery L, Menk AV, Delgoffe GM, Kane LP. Cutting edge: murine mast cells rapidly modulate metabolic pathways essential for distinct effector functions. J. Immunol. 2017; 198:640–644. [PubMed: 27974455]

Pioli PA, Hamilton BJ, Connolly JE, Brewer G, Rigby WF. Lactate dehydrogenase is an AU-rich element-binding protein that directly interacts with AUF1. J. Biol. Chem. 2002; 277:35738–35745. [PubMed: 12107167]

Pollizzi KN, Powell JD. Integrating canonical and metabolic signalling programmes in the regulation of T cell responses. Nat. Rev. Immunol. 2014; 14:435–446. [PubMed: 24962260]

Pollizzi KN, Patel CH, Sun IH, Oh MH, Waickman AT, Wen J, Delgoffe GM, Powell JD. mTORC1 and mTORC2 selectively regulate CD8+ T cell differentiation. J. Clin. Invest. 2015; 125:2090–2108. [PubMed: 25893604]

Powell JD, Delgoffe GM. The mammalian target of rapamycin: linking T cell differentiation, function, and metabolism. Immunity. 2010; 33:301–311. [PubMed: 20870173]

Rathmell JC. Metabolism and autophagy in the immune system: immunometabolism comes of age. Immunol. Rev. 2012; 249:5–13. [PubMed: 22889211]

Rathmell JC, Elstrom RL, Cinalli RM, Thompson CB. Activated Akt promotes increased resting T cell size, CD28-independent T cell growth, and development of autoimmunity and lymphoma. Eur. J. Immunol. 2003; 33:2223–2232. [PubMed: 12884297]

Roos D, Loos JA. Changes in the carbohydrate metabolism of mitogenically stimulated human peripheral lymphocytes. II. Relative importance of glycolysis and oxidative phosphorylation on phytohaemagglutinin stimulation. Exp. Cell Res. 1973; 77:127–135. [PubMed: 4690164]

Scharping NE, Delgoffe GM. Tumor microenvironment metabolism: a new checkpoint for anti-tumor immunity. Vaccines (Basel). 2016; 4:46.

Scharping NE, Menk AV, Moreci RS, Whetstone RD, Dadey RE, Watkins SC, Ferris RL, Delgoffe GM. The tumor microenvironment represses T cell mitochondrial biogenesis to drive intratumoral T cell metabolic insufficiency and dysfunction. Immunity. 2016; 45:374–388. [PubMed: 27496732]

Scharping NE, Menk AV, Whetstone RD, Zeng X, Delgoffe GM. Efficacy of PD-1 blockade is potentiated by metformin-induced reduction of tumor hypoxia. Cancer Immunol. Res. 2017; 5:9–16. [PubMed: 27941003]

Schmidt MM, Rohwedder A, Dringen R. Effects of chlorinated acetates on the glutathione metabolism and on glycolysis of cultured astrocytes. Neurotox. Res. 2011; 19:628–637. [PubMed: 20628842]

Sukumar M, Liu J, Ji Y, Subramanian M, Crompton JG, Yu Z, Roychoudhuri R, Palmer DC, Muranski P, Karoly ED, et al. Inhibiting glycolytic metabolism enhances CD8+ T cell memory and antitumor function. J. Clin. Invest. 2013; 123:4479–4488. [PubMed: 24091329]

van der Windt GJ, O'Sullivan D, Everts B, Huang SC, Buck MD, Curtis JD, Chang CH, Smith AM, Ai T, Faubert B, et al. CD8 memory T cells have a bioenergetic advantage that underlies their rapid recall ability. Proc. Natl. Acad. Sci. USA. 2013; 110:14336–14341. [PubMed: 23940348]

Wieman HL, Wofford JA, Rathmell JC. Cytokine stimulation promotes glucose uptake via phosphatidylinositol-3 kinase/Akt regulation of Glut1 activity and trafficking. Mol. Biol. Cell. 2007; 18:1437–1446. [PubMed: 17301289]

Zhang D, Li J, Wang F, Hu J, Wang S, Sun Y. 2-Deoxy-D-glucose targeting of glucose metabolism in cancer cells as a potential therapy. Cancer Lett. 2014; 355:176–183. [PubMed: 25218591]

Zhang SL, Hu X, Zhang W, Yao H, Tam KY. Development of pyruvate dehydrogenase kinase inhibitors in medicinal chemistry with particular emphasis as anticancer agents. Drug Discov. Today. 2015; 20:1112–1119. [PubMed: 25842042]

Zheng Y, Delgoffe GM, Meyer CF, Chan W, Powell JD. Anergic T cells are metabolically anergic. J. Immunol. 2009; 183:6095–6101. [PubMed: 19841171]

Highlights

- Naive and effector $CD8^+$ T cells induce aerobic glycolysis minutes after activation
- TCR signaling is directly tied to glycolysis via pyruvate dehydrogenase kinase 1 (PDHK1)
- PDHK1-initiated aerobic glycolysis is required for optimal cytokine production
- Cytokine synthesis is controlled via repression of mRNA binding by lactate dehydrogenase

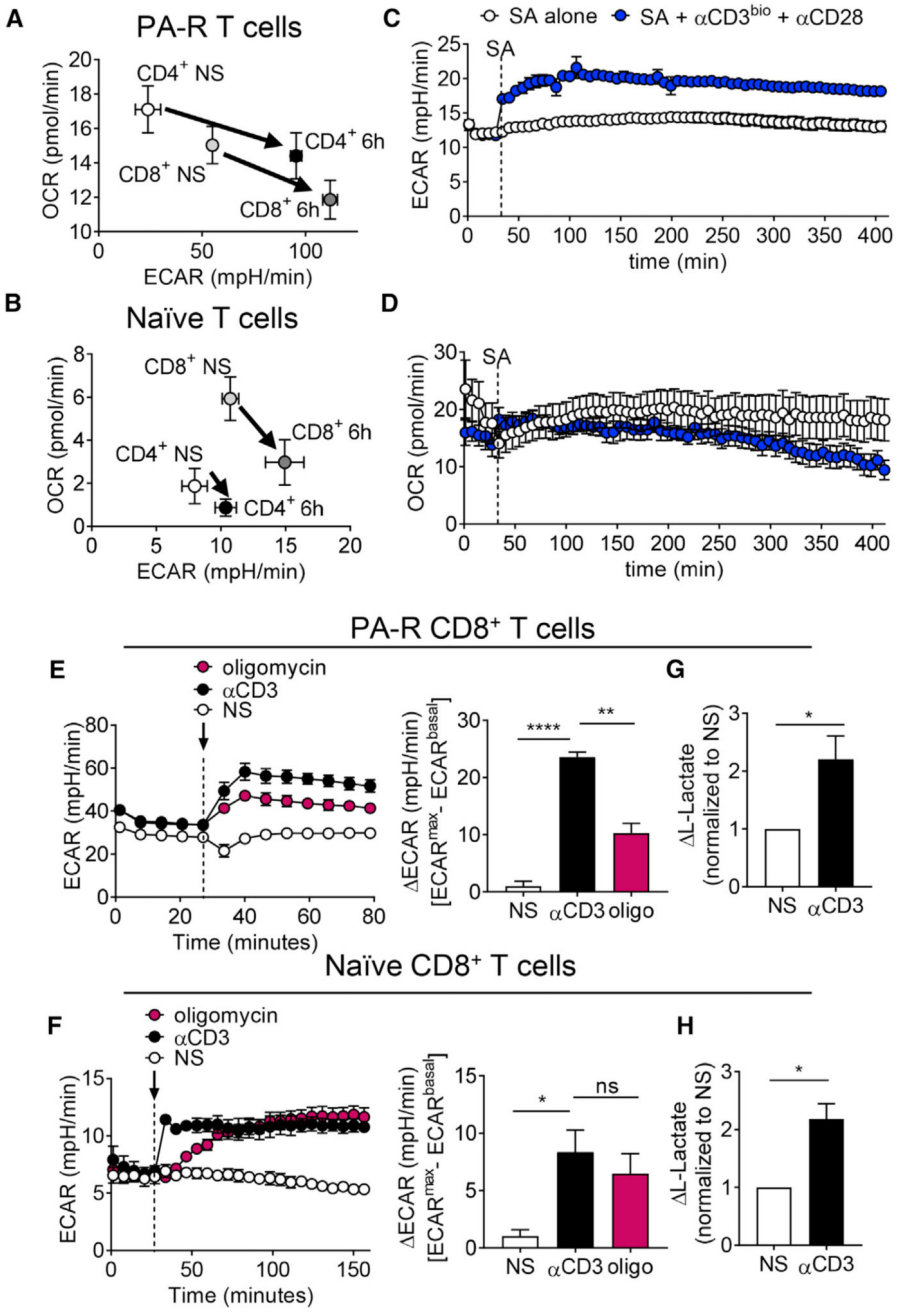

Figure 1. T Cells Rapidly Engage Aerobic Glycolysis upon Activation

(A) Extracellular. acidification rate (ECAR, x axis) and oxygen consumption rate (OCR, y axis) of PA-RT cells (plate-bound αCD3 + CD28 activation and expansion in IL-2) left resting (No Stimulation, NS) or stimulated for 6 hr with 3 μg/mL αCD3 and 2 μg/mL αCD28.

(B) As in (A), but sorted naive ($CD44^{lo}$) T cells.

(C) ECAR trace of naive $CD8^+$ T cells equilibrated in the Seahorse instrument and stimulated via injection of streptavidin or streptavidin-crosslinked αCD3 at 3 μg/mL and soluble αCD28 at 2 μg/mL.

(D) As in (C), but the OCR trace.
(E) ECAR trace (left) and tabulated data (right) of PA-R $CD8^+$ T cells stimulated with streptavidin (NS), streptavidin-crosslinked αCD3, or 1 μM oligomycin (which stimulates glycolytic reserve)
(F) ECAR trace (left) and tabulated data (right) of naive $CD8^+$ T cells stimulated as in (E).
(G) Tabulated L-lactate measurements from PA-R $CD8^+$ T cells stimulated for 1 hr with streptavidin or streptavidin-crosslinked αCD3 at 3 μg/mL.
(H) As in (G), but with naive $CD8^+$ T cells.
Data are representative of 3 independent experiments. *$p < 0.05$, **$p < 0.01$, ***$p < 0.001$. ns, not significant by unpaired t test. Error bars represent SEM.

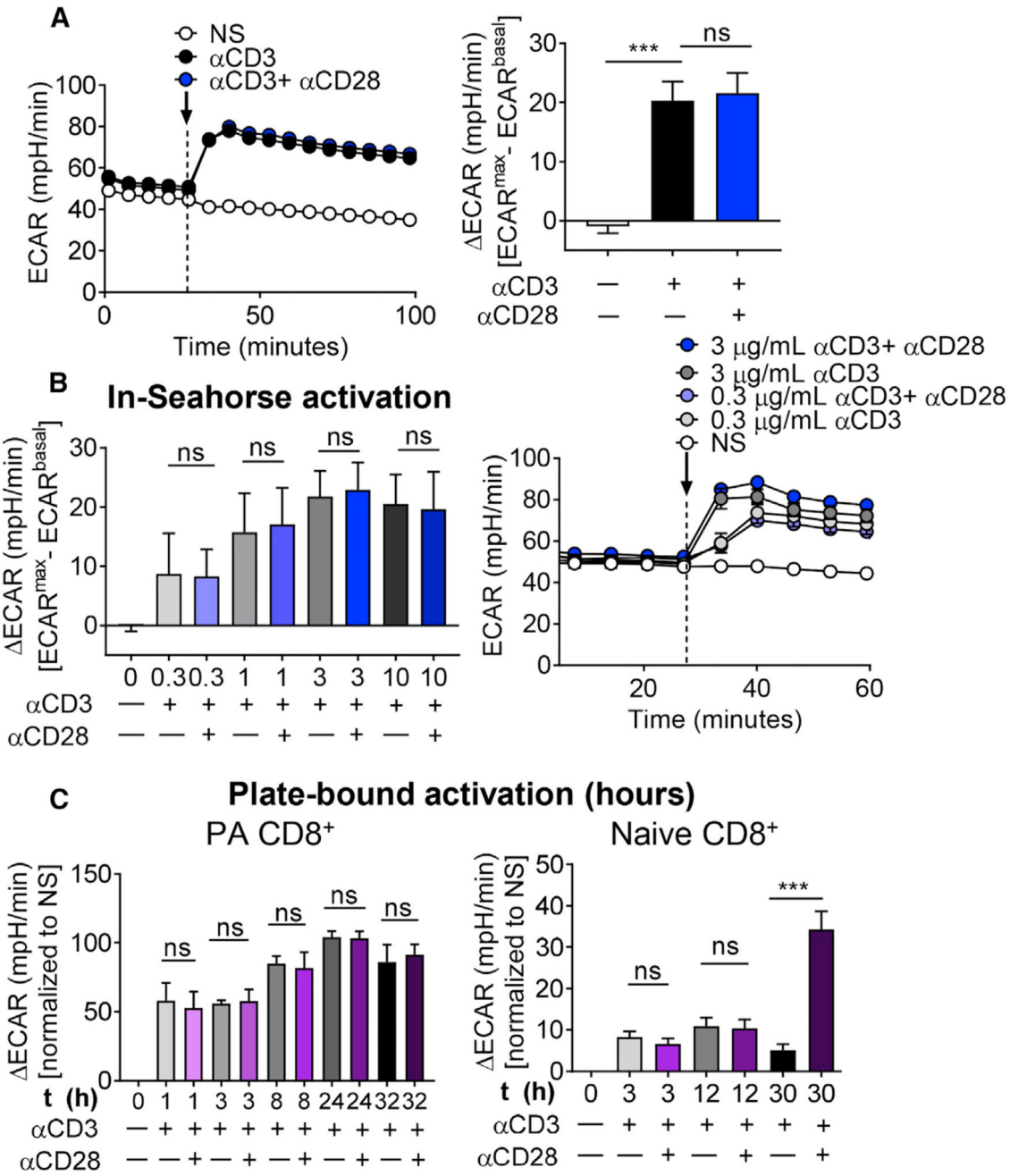

Figure 2. Initiation of Glycolysis in T Cells Is CD28 Independent

(A) ECAR trace of PA-R CD8$^+$ T cells stimulated with streptavidin (No Stimulation, NS) or streptavidin-crosslinked αCD3 at 3 μg/mL in the presence or absence of 2 μg/mL αCD28 (left), and tabulated results (right).

(B) Tabulated ECAR of PA-R CD8$^+$ T cells stimulated with indicated amounts of streptavidin-crosslinked αCD3 in the presence or absence of αCD28 (left), and trace ECAR (right).

(C) Tabulated ECAR levels of PA-R and naive $CD8^+$ T cells stimulated for the indicated times with αCD3 in the presence or absence of 2 μg/mL αCD28 and then assayed in the Seahorse instrument.

Results represent the mean of three (C) or four (A and B) independent experiments. ***$p < 0.001$. ns, not significant by unpaired t test. Error bars represent SEM.

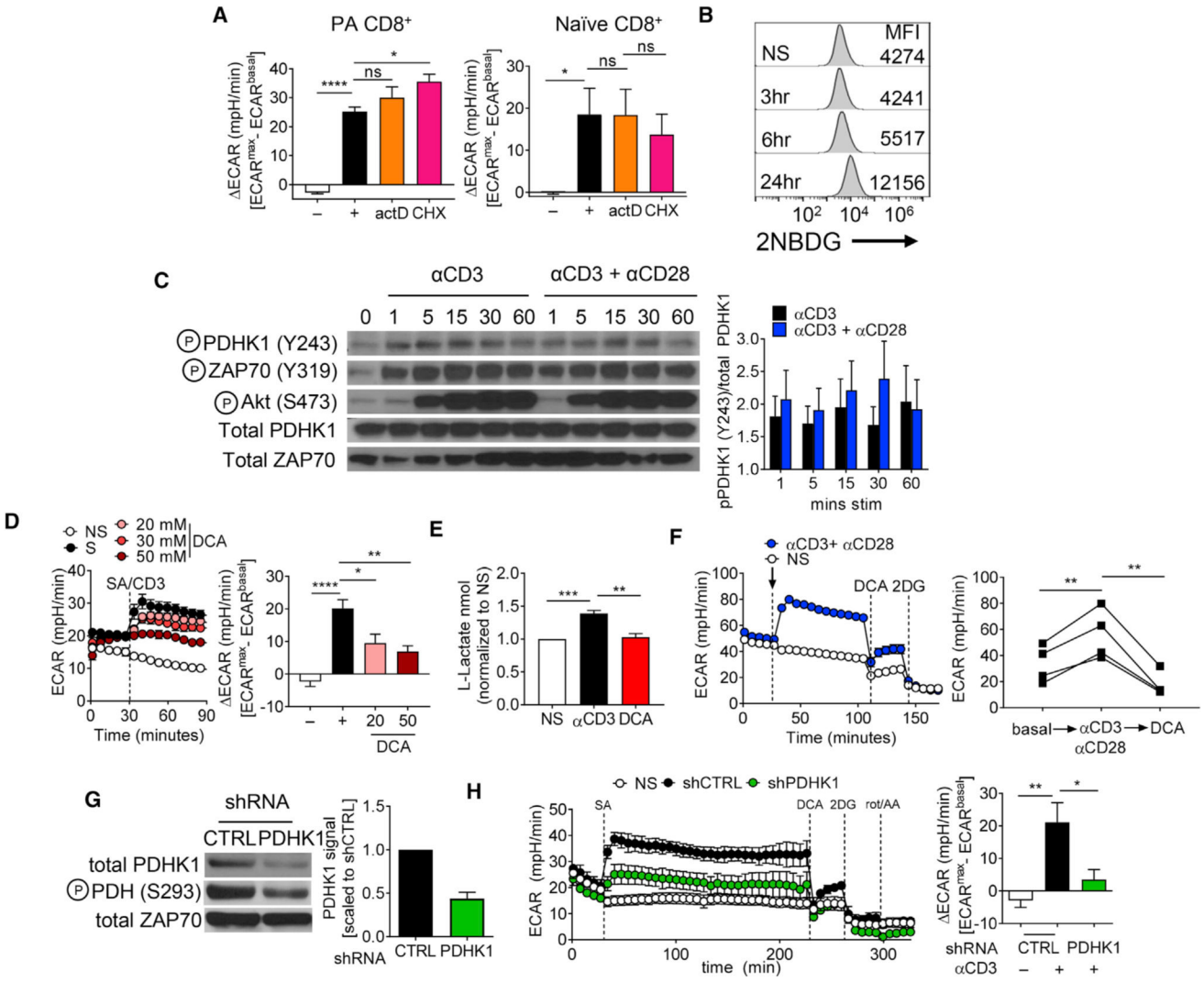

Figure 3. TCR-Induced Aerobic Glycolysis Occurs via PDHK1

(A) Tabulated ECAR of PA-R and naive CD8$^+$ T cells stimulated with streptavidin or streptavidin-crosslinked αCD3 at 3 μg/mL in the presence or absence of transcription or translation inhibition (1 μM actinomycin D [ActD] or 10 μg/mL cycloheximide [CHX]).

(B) Representative histogram of glucose uptake, using PA-R CD8$^+$ T cells reactivated with 3 μg/mL plate-bound αCD3 + 2 μg/mL soluble αCD28 for the indicated times and then pulsed with 2NBDG.

(C) Representative immunoblot (IB) of indicated phospho- or total proteins in lysates from PA-R CD8$^+$ T cells stimulated for the indicated periods with streptavidin or streptavidin-crosslinked αCD3 at 3 μg/mL in the presence of 2 μg/mL αCD28 (left), and tabulated densitometry scanning (right).

(D) ECAR trace of PA-R CD8$^+$ T cells stimulated with streptavidin (No Stimulation, NS) or streptavidin-crosslinked αCD3 at 3 μg/mL and 2 μg/mL αCD28 in the presence or absence of the indicated amounts of dichloroacetate (DCA) (left), and tabulated ECAR (right).

(E) Tabulated L-lactate measurements from PA-R $CD8^+$ T cells stimulated with streptavidin (NS) or streptavidin-crosslinked αCD3 at 3 μg/mL in the presence of absence of 20 mM DCA.

(F) ECAR trace of PA-R $CD8^+$ T cells stimulated as in (D) and then injected with 20 mM DCA (left), and tabulated ECAR (right).

(G) Immunoblot of PDHK1, its enzymatic target pS PDH, and ZAP-70 (as a loading control) from $CD8^+$ T cells retrovirally expressing scrambled control shRNA (shCTRL) or shRNA to *Pdk1* (encoding PDHK1) (left), and tabulated densitometry scanning (right).

(H) ECAR trace of cells from (G) stimulated with crosslinked αCD3 at 3 μg/mL, followed by 20 mM DCA, 10 mM 2-deoxy-d-glucose (2DG), and 500 nM rotenone/antimycin A (left), and tabulated ECAR (right).

Results represent three (A–C, E, and G), four (F and H), or five (D) independent experiments. *$p < 0.05$, **$p < 0.01$, ****$p < 0.0001$ by unpaired t test. ns, not significant. Error bars represent SEM.

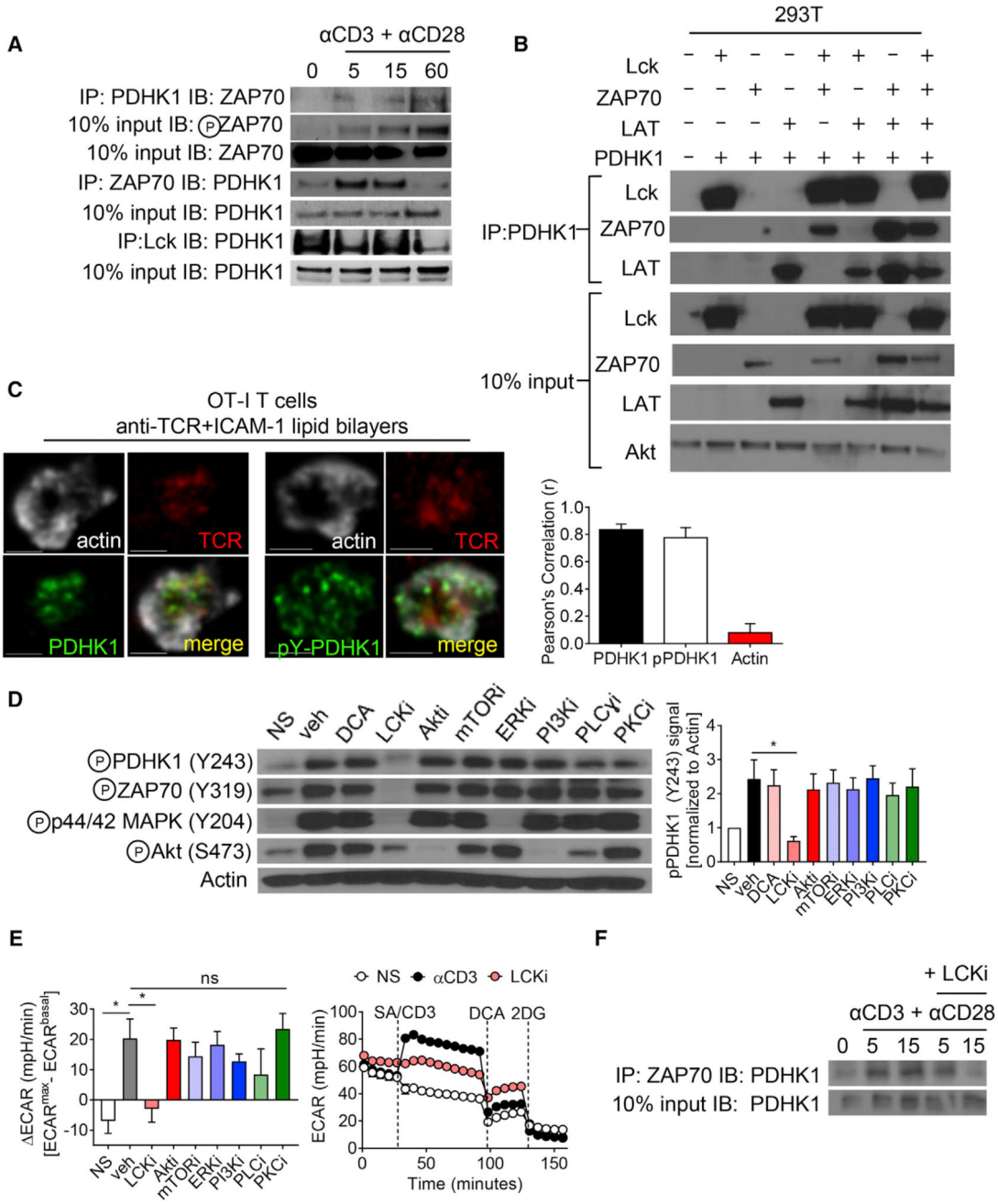

Figure 4. Proximal TCR Signaling Molecules Interact with PDHK1

(A) Immunoblot of immunoprecipitations of the indicated proteins in lysates from $CD8^+$ T cells stimulated with streptavidin or streptavidin-crosslinked αCD3 at 3 μg/mL and αCD28 at 2 μg/mL for the indicated times.

(B) Immunoblot of immunoprecipitations of PDHK1 from HEK293T cells transfected with the indicated combinations of Lck, LAT, ZAP-70, and PDHK1 expression vectors.

(C) TIRF microscopy images of OT-I T cells stimulated on αTCR and ICAM-1 containing stimulatory lipid bilayers for 15 min and then stained intracellularly for total and phospho-PDHK1 (left), and Pearson's correlation in proximity to TCR (right).

(D) Immunoblot of indicated proteins in lysates from PA-R $CD8^+$ T cells stimulated with streptavidin (No Stimulation, NS) or streptavidin-crosslinked αCD3 at 3 μg/mL in the presence or absence of the indicated inhibitors (left), and tabulated densitometry (right).
(E) Tabulated ECAR of PA-R $CD8^+$ T cells stimulated as in (D) in the presence or absence of the indicated inhibitors (left), and trace ECAR of Lck inhibition (right).
(F) Immunoblot of immunoprecipitations of the indicated proteins in lysates from PA-R $CD8^+$ T cells stimulated as in (A) for the indicated times in the presence or absence of 10 nM Lck inhibitor.
Results represent the mean of three (A, D, and F), four (B), five (E), or seven (C) independent experiments. *$p < 0.05$ by unpaired t test. ns, not significant. Error bars represent SEM.

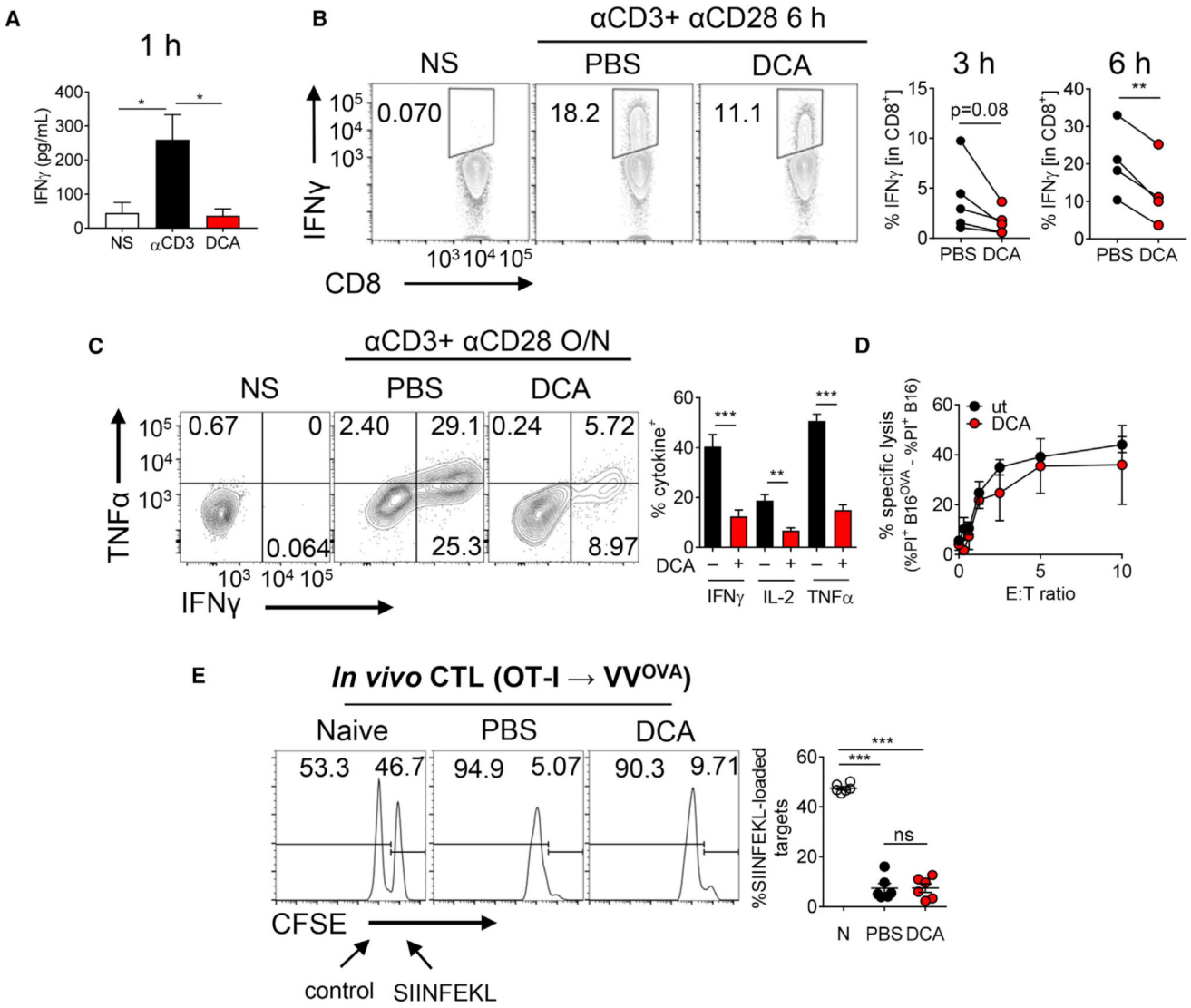

Figure 5. PDHK1-Mediated Glycolysis Is Required for Cytokine Production but Dispensable for Cytotoxic T Cell Function

(A) Tabulated IFNγ ELISA data from PA-R $CD8^+$ T cells, in which cells were pretreated with 20mMDCA 30 min before 1-hr activation via streptavidin-crosslinked αCD3 at 3 μg/mL.

(B) Representative flow cytogram (left) and tabulated cytokine production (right) from PA-R $CD8^+$ T cells stimulated for 6 hr with 3 μg/mL αCD3 and 2 μg/mL αCD28 in the presence or absence of 20 mM DCA.

(C) Representative flow cytogram (left) and tabulated cytokine production (right) from PA-R $CD8^+$ T cells stimulated overnight with 3 μg/mL αCD3 and 2 μg/mL αCD28 in the presence or absence of 5 mM DCA.

(D) Quantified *in vitro* cytotoxicity assay using PA-R OT-I T cells cultured with OVA-expressing or parental B16 melanoma cells in the presence or absence of 5 mM DCA.

(E) Representative cytogram (left) and tabulated results (right) of an *in vivo* cytotoxicity assay in which OT-I cytotoxic T lymphocyte (CTL) were generated *in vivo* with vaccinia

virus (VV)^{OVA}, after which mice receive an adoptive transfer of control or cognate-peptide-loaded splenocyte targets differentially labeled with CFSE and an immunoprecipitation (IP) injection of either PBS or DCA.

Results represent the mean of five (C), four (B), or three (A, D, and E) independent experiments. *$p < 0.05$, **$p < 0.01$, ***$p < 0.001$ by unpaired t test. Error bars represent SEM.

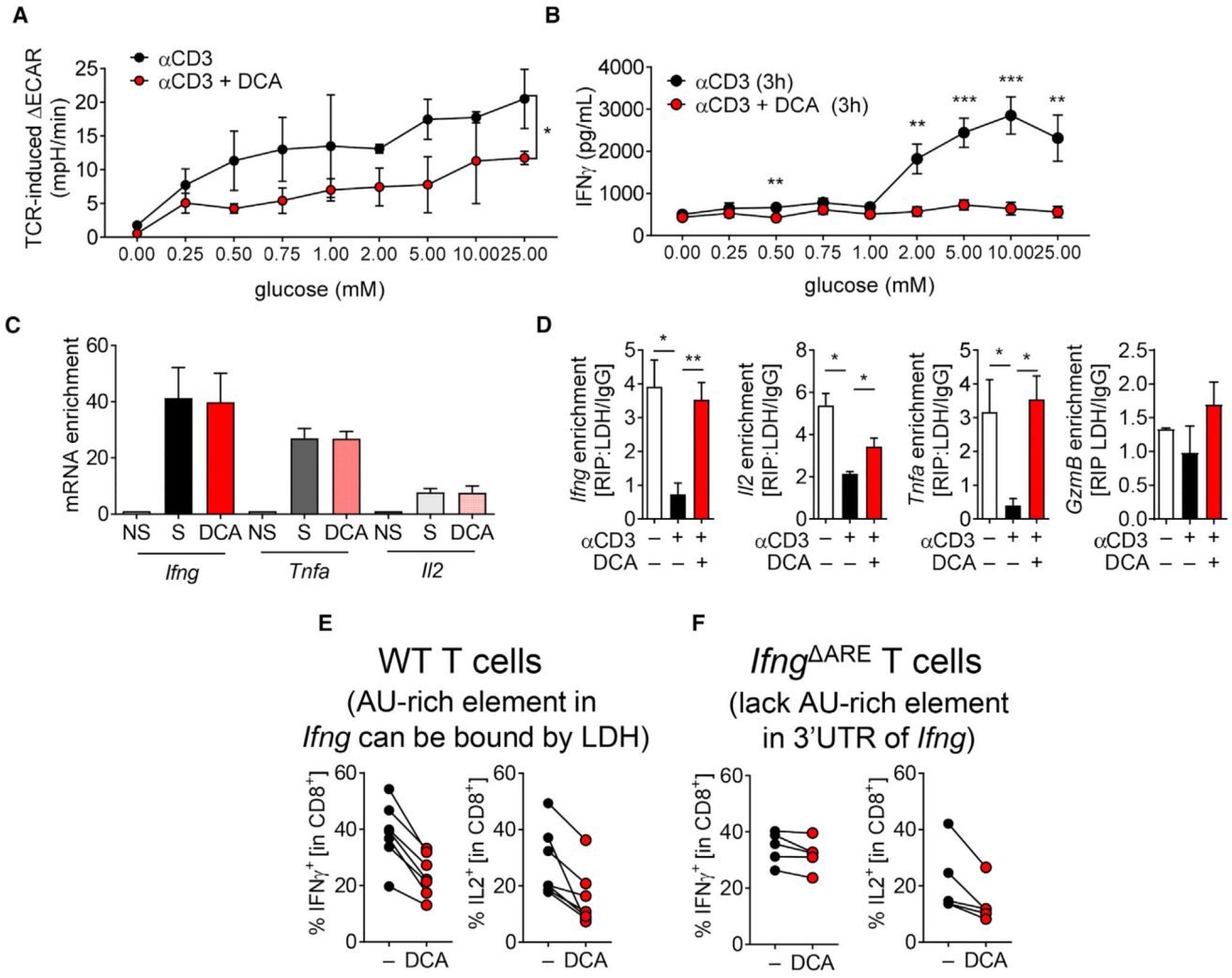

Figure 6. PDHK1-Mediated Aerobic Glycolysis Integrates Glucose Availability and LDH Activity to Control Cytokine Synthesis at the Post-transcriptional Level

(A) Tabulated ECAR generated from PA-R $CD8^+$ T cells stimulated with streptavidin or streptavidin-crosslinked αCD3 at 3 μg/mL in the presence or absence of 20 mM DCA in the indicated concentration of glucose.

(B) IFNγ production from supernatant collected from the flux analysis experiment in (A) measured by ELISA.

(C) qPCR analysis of cDNA generated from RNA extracted from PA-R $CD8^+$ T cells stimulated overnight with 3 μg/mL αCD3 and 2 μg/mL αCD28 in the presence or absence of DCA. mRNA levels of the indicated cytokines were standardized with *Actb* expression.

(D) qPCR analysis of cDNA generated from RNA IP using LDHA-specific antibodies or a species-specific control. Precipitates were prepared from PA-R $CD8^+$ T cells left resting or stimulated with 3 μg/mL αCD3 and 2 μg/mL αCD28 in the presence or absence of DCA overnight and then crosslinked with 1% formaldehyde before RNA IP. Results are expressed as fold enrichment over species-specific control (IgG).

(E) IFNγ and IL-2 production (measured by flow cytometry) of WT $CD8^+$ T cells stimulated with 3 μg/mL αCD3 and 2 μg/mL αCD28 in the presence of DCA.

(F) IFNγ and IL-2 production of T cells stimulated with 3 μg/mL αCD3 and 2 μg/mL αCD28 from mice homozygous for a targeted deletion of the *Ifng* AU-rich element (ARE) (ΔA) or littermate controls.

Results represent the mean of three (A–D) or two (E and F) (n = 5–7 mice per group) independent experiments. *$p < 0.05$, **$p < 0.01$, ***$p < 0.001$ by two-way ANOVA (A) unpaired t test (B–F). Error bars represent SEM.